Gaseous ^{3}He-^{3}He magnetic dipolar spin relaxation

N. R. Newbury, A. S. Barton, G. D. Cates, W. Happer, and H. Middleton
Department of Physics, Princeton University, Princeton, New Jersey 08544
(Received 10 December 1992)

We derive the nuclear-spin-relaxation rate of gaseous ^{3}He due to the magnetic-dipole interaction between the ^{3}He nuclear spins. This dipolar relaxation rate is numerically evaluated for temperatures from 0.1 to 550 K. At room temperature, the relaxation time for a ^{3}He density of 10 amagats is 74.4 h. We have made a series of high-density (4–12 amagat) ^{3}He samples for which nuclear relaxation is limited by the magnetic-dipole interaction. Both our theoretical and experimental results are particularly important for the growing use of ^{3}He, polarized through spin exchange with optically pumped Rb vapor.

PACS number(s): 34.50.Pi, 33.25.Bn, 32.80.Bx

I. INTRODUCTION

The relaxation of nuclear-spin-polarized ^{3}He gas has attracted considerable interest since the early pioneering work in the field [1–3]. Until recently ^{3}He nuclear relaxation at room temperature was dominated by wall effects or magnetic-field inhomogeneities [4]. However, we are now consistently able to produce ^{3}He samples with relaxation rates close to a fundamental limit imposed by the magnetic-dipole–dipole coupling between ^{3}He nuclear spins. In a binary collision between two ^{3}He atoms, the magnetic-dipole interaction couples the nuclear spins to the relative angular momentum of the ^{3}He atoms. As a result, nuclear polarization is lost to orbital angular momentum. In this paper we present a theoretical derivation of the dipolar spin-relaxation rate, numerical results for the spin relaxation of ^{3}He, and experimental results demonstrating that the relaxation of our samples is limited by dipolar spin relaxation.

Long ^{3}He nuclear-spin-relaxation times are important for the growing use of ^{3}He samples polarized through spin exchange with a polarized alkali-metal vapor, typically Rb. In a recent experiment at the Stanford Linear Accelerator Center, polarized electrons were scattered from an 8 atm ^{3}He target to resolve outstanding questions regarding the spin-structure function of the neutron [5]. In nuclear physics, polarized ^{3}He targets have been employed to polarize neutrons [6, 7], examine the electromagnetic form factor of the neutron [8], and explore spin-dependent pion-nucleon scattering [9]. Finally, several atomic physics experiments have used polarized ^{3}He [10, 11], the most exotic of these being the formation of polarized muonic ^{3}He [12]. Long spin-relaxation times are of practical importance for two reasons. First, in these experiments, as well as in the experiment described here, the ^{3}He is polarized through spin exchange with optically pumped alkali-metal vapor (typically Rb) [4, 13, 14]. For a spin-exchange rate $\gamma_{\rm SE}$, the ^{3}He polarization will saturate at a value

$$P_{\rm He} = \frac{\gamma_{\rm SE}}{\gamma_{\rm SE} + \Gamma} P_A, \tag{1}$$

where P_A is the average alkali-metal polarization and Γ is the contribution to the ^{3}He relaxation from all mechanisms other than alkali-metal–^{3}He spin exchange. At typical Rb number densities of 5×10^{14} cm^{-3}, $\gamma_{\rm SE} \sim 0.3$ h s^{-1} [4]. High polarizations can only result if $\Gamma \ll \gamma_{\rm SE}$. Second, long relaxation times allow one to polarize the ^{3}He sample prior to and in a different location than the experiment. This approach was taken in Ref. [12] and can allow for a great simplification of the experimental apparatus.

We derive the spin relaxation caused by the dipole-dipole interaction using spherical basis tensors and assuming only binary collisions. Since we consider a rather general form of a spin-dependent scattering potential, the derivation should also serve as a mathematical framework for spin-dependent scattering. In the Appendix, we give a particularly simple expression for the dipolar spin relaxation of a gas of spin-1/2 noninteracting Fermions.

We have numerically evaluated the expression for dipolar spin relaxation for temperatures from 0.1 to 550 K using three different ^{3}He-^{3}He interatomic potentials. At room temperature (23 °C), the dipolar relaxation rate is

$$\frac{1}{\tau} = \frac{[^3{\rm He}]}{744} {\rm h\,s^{-1}}, \tag{2}$$

where $[^3$He$]$ is the ^{3}He density in amagats. (An amagat is a unit of density corresponding to 1 atm at 0 °C.) Although these relaxation times are very long, we have successfully produced glass cells containing 4–12 amagats of ^{3}He in which the spin relaxation is completely dominated by dipolar relaxation.

The relaxation of polarized ^{3}He at low temperatures has received considerable attention [15] because of interest in studying the transport properties of a polarized Fermi gas [16]. Bulk dipolar relaxation has been observed at temperatures from 1.7 to 19 K [17, 18]. Motivated by these measurements, Shizgal derived an expression, similar but not identical to ours, for the dipolar relaxation of ^{3}He based on the generalized Boltzmann transport equation [19, 20]. In this early work, it was suggested that the relaxation rate could be used to constrain the empirical He-He interatomic potential [18, 20], as has been done by Aziz, McCourt, and Wong [21]. Recently, Mullin, Lakoë, and Richards [22] derived an expression for the relaxation rate which agrees with our result.

We briefly mention two other possible intrinsic bulk relaxation mechanisms for a spin-1/2 gas. The first is relaxation due to the spin-rotation interaction. While this relaxation dominates in polarized ^{129}Xe [23], it is expected to be small for polarized ^{3}He [18]. This expectation is confirmed by the small difference between our measured relaxation rates and the theoretical dipolar limit. The second is relaxation caused by the existence of a permanent electric dipole moment (EDM) associated with the spin. In fact, the relaxation of a spin-1/2 gas has been considered as a candidate for a nuclear EDM search [24]. However, Purcell showed [24] that the standard simple estimate of the relaxation rate from an EDM [25] is many orders of magnitude too large because the electric field experienced by the nucleus in successive collisions is strongly correlated. As a result, the relaxation rate for our ^{3}He cells is extremely insensitive to the existence of a ^{3} nuclear EDM.

II. THEORY

A. Introduction

We are interested in solving for the nuclear-spin relaxation of ^{3}He due to the dipolar interaction

$$V^{(1)} = \left(\frac{\mu_I}{I}\right)^2 \frac{1}{r^3}\left(\mathbf{I}_1\cdot\mathbf{I}_2 - \frac{3(\mathbf{I}_1\cdot\mathbf{r})(\mathbf{r}\cdot\mathbf{I}_2)}{r^2}\right) \tag{3}$$

between the nuclear spins $\mathbf{I}_1$ and $\mathbf{I}_2$ of a pair of ^{3}He atoms, separated by $\mathbf{r}$. The ^{3}He nuclear magnetic moment is μ_I. We consider only binary collisions, so that the colliding pair can be represented in the center-of-mass frame by a pseudoparticle with spin

$$\mathbf{S} = \mathbf{I}_1 + \mathbf{I}_2. \tag{4}$$

The problem of ^{3}He relaxation can then be cast in the more general form of solving for the relaxation of particles of spin S which are scattered by the potential

$$V = V^{(0)}(r) + \lambda V^{(1)}(\mathbf{r}), \tag{5}$$

located at the origin of a coordinate system. In the case of ^{3}He-^{3}He scattering, the spin-independent potential $V^{(0)}(r)$ is the interatomic potential. We have inserted a perturbation parameter λ in (5), which we use to keep track of the various orders of perturbation theory.

Generally, we can write the noncentral spin-dependent perturbing potential as

$$V^{(1)} = R(r)Y_L(\hat{\mathbf{r}})\cdot T_L(SS), \tag{6}$$

which describes the interaction of the 2^L-pole moment of the spin S with the scattering center. The generalized dot product between spherical tensors is

$$Y_L(\hat{\mathbf{r}})\cdot T_L(SS) \equiv \sum_{M=-L}^{L}(-1)^M Y_{LM}(\hat{\mathbf{r}})T_{L,-M}(SS) \equiv (-1)^L\sqrt{2L+1}\left[Y_L(\hat{\mathbf{r}})T_L\right]_{00}, \tag{7}$$

where the coupling operation indicated by square brackets is defined by (8) below. The spin dependence is described by the spherical basis tensor [26–30]

$$T_{LM}(SS') = \left[|S\rangle\{S'|\right]_{LM} = \sum_{\mu}|S,\mu\rangle\{S',M-\mu|\,C(SS'L;\mu,M-\mu)\,, \tag{8}$$

where the sum on μ extends over all allowed values of the Clebsch-Gordan coefficient C and $|S,\mu\rangle$ is the spin substate of the particle with azimuthal angular momentum $\mu = -S, -S+1, \ldots, S$. We use a curly bracket to denote a bra vector

$$\{S,\mu| = \langle S,-\mu|\,(-1)^{\mu+S}\,. \tag{9}$$

Specifically, the dipole-dipole interaction (3) can be rewritten in the form of (6) as

$$V^{(1)} = R(r)Y_2(\hat{\mathbf{r}})\cdot T_2(11), \tag{10}$$

where the radial function is

$$R(r) = -\sqrt{\frac{6\pi}{5}}\left(\frac{\mu_I}{I}\right)^2\frac{1}{r^3}. \tag{11}$$

The dipole-dipole interaction (10) is a triplet-space operator. It can cause transitions between the azimuthal sublevels of the triplet space, but it cannot couple triplet and singlet components of the wave function.

We will solve below for the general case of spin relaxation due to a potential of the form (6). Using the general expression derived, we then calculate the relaxation rate for a dipolar interaction (10).

B. Spin currents

For the present, we will ignore the symmetry constraints for identical particles and make the appropriate modifications for identical fermions in Sec. II F. The density matrix ρ describing the state of a particle (or pseudoparticle representing a pair of colliding particles) satisfies

$$\frac{\partial\rho}{\partial t} + \nabla\cdot\mathbf{j} = \frac{1}{i\hbar}[V,\rho]. \tag{12}$$

The probability current density operator is

$$\mathbf{j} = \frac{\hbar}{2mi}\left(|\nabla\psi\rangle\langle\psi| - |\psi\rangle\langle\nabla\psi|\right), \tag{13}$$

where m is the mass of the particle or pseudoparticle and $|\psi\rangle$ is its wave function.

If we define the probability Q by

$$Q = \int \rho d^3\mathbf{r}, \tag{14}$$

the rate of change of $\mathbf{S}$ will be

$$\frac{d}{dt}\langle \mathbf{S}\rangle = \mathrm{Tr}\{\mathbf{S}\dot{Q}\}, \tag{15}$$

where $\dot{Q} \equiv dQ/dt$.

Let us define a spherical source volume Ω_S of radius s such that the scattering potential is negligibly small outside of Ω_S. If we assume ρ has reached a steady state within Ω_S, we can use (12) to find

$$\dot{Q} = \int_{\Omega_S} \mathbf{j}\cdot d\mathbf{A}, \tag{16}$$

where the integral is over the surface of Ω_S. Once the current density $\mathbf{j}$ on the surface of the scattering volume is known, we can calculate $\dot{Q}$ from (16), and from (15) find the spin-relaxation rate.

C. Modified optical theorem

The scattering state with the proper asymptotic behavior and momentum $\hbar\mathbf{k}$ is

$$|\psi_{\mathbf{k}}\rangle \equiv \sum_{\nu} |\nu\rangle\psi_{\mathbf{k}\mu}(\mathbf{r},\nu)\langle\mu|\chi\rangle \sim \left(e^{i\mathbf{k}\cdot\mathbf{r}} + \frac{e^{ikr}}{r} f(\hat{\mathbf{k}}',\hat{\mathbf{k}})\right)|\chi\rangle, \tag{17}$$

where the direction of the scattered wave is $\hat{\mathbf{k}}' = \hat{\mathbf{r}}$ and $|\mu\rangle$ describes the spin substate. We have introduced a coherent, initial spin state $|\chi\rangle = \sum_\mu |\mu\rangle\langle\mu|\chi\rangle$ of the incoming particle. The expression in parentheses on the right-hand side is formally the same as the expression for the asymptotic probability amplitude for a spinless particle, but f is to be interpreted as a spin operator,

$$f = \sum_{\nu\mu} |\nu\rangle f_{\nu,\mu}\langle\mu| = \sum_j f_j \cdot T_j(SS). \tag{18}$$

Substituting the scattering state (17) into the definition of the current density (13), we find the probability current (16) for a specific $\mathbf{k}$ is

$$\dot{Q}_{\mathbf{k}} = \frac{2\pi i\hbar}{m}\left(\bar{f}|\chi\rangle\langle\chi| - |\chi\rangle\langle\chi|\bar{f}^\dagger\right) + \frac{\hbar k}{m}\int f|\chi\rangle\langle\chi|f^\dagger d^2\hat{\mathbf{k}}', \tag{19}$$

where the forward scattering amplitude $\bar{f} = f(\hat{\mathbf{k}},\hat{\mathbf{k}})$. In writing (19), we have used

$$\int f(\hat{\mathbf{k}}',\hat{\mathbf{k}})e^{iks(1-\hat{\mathbf{k}}\cdot\hat{\mathbf{k}}')}(1+\hat{\mathbf{k}}\cdot\hat{\mathbf{k}}')d^2\hat{\mathbf{k}}' \sim \frac{4\pi i}{ks}\bar{f}, \tag{20}$$

because the integrand will oscillate rapidly for all but the forward scattering direction ($\hat{\mathbf{k}}' \approx \hat{\mathbf{k}}$) as $ks \to \infty$. Equation (19) is the familiar optical theorem, generalized to particles with spin. The first term accounts for the forward scattering and the second accounts for the lateral scattering.

D. Distorted-wave Born approximation

So far we have made no assumptions about the magnitude of the scattering potentials, but we will now assume that $V^{(1)}$ is small compared to $V^{(0)}$. This is the case for the dipole-dipole interaction, which is some eight orders smaller than the spin-independent potential which accounts for momentum-changing collisions.

The time-independent Schrödinger equation for the particle is

$$\left(\frac{-\hbar^2}{2m}\nabla^2 + V^{(0)} + \lambda V^{(1)} - \frac{\hbar^2k^2}{2m}\right)|\psi_{\mathbf{k}}\rangle = 0. \tag{21}$$

The solution to (21) can be written as a distorted-wave Born series

$$|\psi_{\mathbf{k}}\rangle = |\psi_{\mathbf{k}}^{(0)}\rangle + \lambda|\psi_{\mathbf{k}}^{(1)}\rangle + \lambda^2|\psi_{\mathbf{k}}^{(2)}\rangle + \cdots. \tag{22}$$

Similarly, the scattering amplitude will be

$$f = f^{(0)} + \lambda f^{(1)} + \lambda^2 f^{(2)} + \cdots \tag{23}$$

and the current (16) will be

$$\dot{Q} = \dot{Q}^{(0)} + \lambda\dot{Q}^{(1)} + \lambda^2\dot{Q}^{(2)} + \cdots. \tag{24}$$

Because of the rotational invariance of the potential V, each term of the Born expansion of f must be invariant to simultaneous rotations of $\mathbf{r}$, $\mathbf{k}$, and $\mathbf{S}$. Thus, the scattering amplitudes must have the form

$$f^{(n)} = \sum_{l',l,j} f_{l'lj}^{(n)}[Y_{l'}(\hat{\mathbf{k}}')Y_l(\hat{\mathbf{k}})]_j \cdot T_j. \tag{25}$$

Physically, the term labeled $l'lj$ in the sum (25) represents the scattering of the lth partial wave of the incident beam into an outgoing spherical wave of angular momentum l'. At the same time, the tensor T_j ensures that the azimuthal quantum number of the particle's spin changes enough to conserve angular momentum.

Using the addition formula for spherical harmonics, we readily show that the nth-order forward scattering amplitude is

$$\bar{f}^{(n)} = \sum_{l',l,j} f_{l'lj}^{(n)}\sqrt{\frac{(2l'+1)(2l+1)}{4\pi(2j+1)}}C(l'lj;00)Y_j(\hat{\mathbf{k}})\cdot T_j. \tag{26}$$

Following the usual derivation of the distorted-wave Born approximation (DWBA) [31], we can find the zeroth- and first-order contributions to the scattering amplitude f. We write the zeroth-order wave function as the simple product of a spin function and a spatial function

$$|\psi_{\mathbf{k}}^{(0)}\rangle = \phi_{\mathbf{k}}^{+}(\mathbf{r})|\chi\rangle. \tag{27}$$

The solutions $\phi_{\mathbf{k}}^{\pm}$ have the partial wave expansions

$$\phi_{\mathbf{k}}^{\pm}(\mathbf{r}) = 4\pi \sum_l i^l e^{\pm i\delta_l} \frac{g_l(r)}{kr} Y_l(\hat{\mathbf{k}}') \cdot Y_l(\hat{\mathbf{k}}) \tag{28}$$

$$\sim e^{i\mathbf{k}\cdot\mathbf{r}} + \frac{e^{\pm ikr}}{r} f^{\pm}.$$

The radial wave functions g_l of (28) obey the radial Schrödinger equation

$$\left(-\frac{d^2}{dr^2} + \frac{l(l+1)}{r^2} + \frac{2m}{\hbar^2} V^{(0)}(r) - k^2\right) g_l(r) = 0 \tag{29}$$

and they satisfy the boundary conditions

$$g_l \underset{r\to 0}{\longrightarrow} 0, \tag{30}$$

$$g_l \underset{r\to\infty}{\sim} \sin\left(kr - \frac{\pi l}{2} + \delta_l\right). \tag{31}$$

The phase shifts δ_l of (30) determine the zeroth-order spin-independent scattering amplitude

$$f^+(\hat{\mathbf{r}}, \hat{\mathbf{k}}) = \frac{2\pi}{ik} \sum_l (e^{2i\delta_l} - 1) Y_l(\hat{\mathbf{k}}') \cdot Y_l(\hat{\mathbf{k}}),$$

$$f^-(\hat{\mathbf{r}}, \hat{\mathbf{k}}) = \{f^+(\hat{\mathbf{r}}, -\hat{\mathbf{k}})\}^*. \tag{32}$$

Since the scattering state (17) has an outgoing spherical wave, the zeroth-order scattering amplitude is

$$f^{(0)} = f^+. \tag{33}$$

The standard result of the DWBA [31] is that the first-order scattering amplitude is given by

$$f^{(1)} = \frac{-m}{2\pi\hbar^2} \int \phi_{\mathbf{k}'}^{-*}(\mathbf{r}') V^{(1)}(\mathbf{r}') \phi_{\mathbf{k}}^{+}(\mathbf{r}') d^3\mathbf{r}'. \tag{34}$$

Substituting in the partial-wave expansions (28) for $\phi_{\mathbf{k}}^{+}(\mathbf{r}')$ and $\phi_{\mathbf{k}'}^{-}(\mathbf{r}')$ and carrying out the angular and radial integrals, we find the tensor coefficient of the first-order scattering amplitude to be

$$f_{l'lj}^{(1)} = \frac{-2m}{\hbar^2 k^3} R_{l'l}\, i^{(l'+l)} e^{i(\delta_{l'}+\delta_l)} \sqrt{4\pi(2l'+1)} \times C(l'Ll;00)\delta_{j,L}, \tag{35}$$

where the radial matrix element is

$$R_{l'l} = \int_0^\infty g_{l'}(r) g_l(r) R(r)\, k\, dr. \tag{36}$$

To first order, (35) shows that the spin-dependent potential can change the orbital angular momentum of the particle by as many as L units.

E. General spin relaxation

Substituting the expansion for the current (23) into the modified optical theorem (19), we find the three lowest-order contributions to the probability current:

$$\dot{Q}_{\mathbf{k}}^{(0)} = \frac{2\pi i\hbar}{m}\left(\bar{f}^{(0)}|\chi\rangle\langle\chi| - |\chi\rangle\langle\chi|\bar{f}^{(0)\dagger}\right) + \frac{\hbar k}{m}\int f^{(0)}|\chi\rangle\langle\chi|f^{(0)\dagger} d^2\hat{\mathbf{k}}', \tag{37}$$

$$\dot{Q}_{\mathbf{k}}^{(1)} = \frac{2\pi i\hbar}{m}\left(\bar{f}^{(1)}|\chi\rangle\langle\chi| - |\chi\rangle\langle\chi|\bar{f}^{(1)\dagger}\right) + \frac{\hbar k}{m}\int \left(f^{(0)}|\chi\rangle\langle\chi|f^{(1)\dagger} + f^{(1)}|\chi\rangle\langle\chi|f^{(0)\dagger}\right) d^2\hat{\mathbf{k}}',$$

$$\dot{Q}_{\mathbf{k}}^{(2)} = \frac{2\pi i\hbar}{m}\left(\bar{f}^{(2)}|\chi\rangle\langle\chi| - |\chi\rangle\langle\chi|\bar{f}^{(2)\dagger}\right) + \frac{\hbar k}{m}\int \left(f^{(0)}|\chi\rangle\langle\chi|f^{(2)\dagger}\right. \tag{38}$$

$$\left. + f^{(2)}|\chi\rangle\langle\chi|f^{(0)\dagger}\right) d^2\hat{\mathbf{k}}' + \frac{\hbar k}{m}\int f^{(1)}|\chi\rangle\langle\chi|f^{(1)\dagger} d^2\hat{\mathbf{k}}'. \tag{39}$$

Using the zeroth-order scattering amplitude (33), one can verify that $\dot{Q}_{\mathbf{k}}^{(0)} = 0$ (i.e., the spin-independent potential produces no probability current between the spin sublevels).

We are interested in spin relaxation for gaseous samples in thermal equilibrium, for which the distribution of $\hbar\mathbf{k}$ is isotropic. We therefore define an angle-averaged current by

$$\dot{Q}^{(n)} = \frac{1}{4\pi}\int \dot{Q}_{\mathbf{k}}^{(n)}\, d^2\hat{\mathbf{k}}. \tag{40}$$

Noting the δ function in (35), we find $\dot{Q}^{(1)} = 0$ since the average value of $Y_{LM}(\hat{\mathbf{k}})$ is zero.

We use (25), (26), (33), the δ function in (35), and (39) to calculate the angle-averaged, second-order probability current

$$\dot{Q}^{(2)} = \frac{\hbar k}{m}\left\{ \frac{1}{2k}\sum_l (-1)^l \sqrt{\frac{2L+1}{2S+1}} \times \left(ie^{-2i\delta_l} f_{ll0}^{(2)} + \text{c.c.}\right)|\chi\rangle\langle\chi| + \frac{1}{4\pi}\sum_{l',l}\left|f_{l'lL}^{(1)}\right|^2 T_L \cdot |\chi\rangle\langle\chi| T_L\right\}, \tag{41}$$

where c.c. is the complex conjugate of the preceding expression. Since the total number of particles is conserved, the trace of the probability current of any order must vanish, so

$$\mathrm{Tr}\,\{\dot{Q}^{(2)}\} = \frac{\hbar k}{m}\Bigg\{ \frac{1}{2k}\sum_l (-1)^l \sqrt{\frac{2L+1}{2S+1}} \times \left(ie^{-2i\delta_l} f^{(2)}_{ll0} + \text{c.c.}\right) + \frac{1}{4\pi}\sum_{l',l} \left|f^{(1)}_{l'lL}\right|^2 \frac{2L+1}{2S+1}\Bigg\} = 0. \quad (42)$$

We have used the identity, analogous to the addition formula for spherical harmonics,

$$T_L \cdot T_L = \frac{2L+1}{2S+1}. \quad (43)$$

We can eliminate the second-order scattering amplitudes from (41) with the aid of (42) to find

$$\dot{Q}^{(2)} = \frac{\hbar k}{4\pi m}\sum_{l',l}\left|f^{(1)}_{l'lL}\right|^2 \left\{T_L\cdot|\chi\rangle\langle\chi|T_L - \frac{2L+1}{2S+1}|\chi\rangle\langle\chi|\right\}. \quad (44)$$

Using this expression and the tensor identity

$$T_L \cdot \mathbf{S} T_L = (2L+1)W(LSS1;SS)\mathbf{S}, \quad (45)$$

where W denotes a Racah coefficient, Eq. (15) becomes

$$\frac{d}{dt}\langle\mathbf{S}\rangle = -\frac{1}{\tau_k}\langle\mathbf{S}\rangle, \quad (46)$$

where the spin-relaxation rate due to isotropic collisions with relative momentum $\hbar k$ is

$$\frac{1}{\tau_k} = [N]\frac{2m}{\hbar^3 k^5}\frac{L(L+1)}{S(S+1)(2S+1)} \times \sum_{l',l}(2l'+1)(2l+1)C^2(l'lL;00)R^2_{l'l}. \quad (47)$$

We have used the explicit values (35) of $f^{(1)}_{l'lL}$ and the algebraic formula for the Racah coefficient to write (47). We have also introduced the number density $[N]$ of scatterers. We implicitly assumed $[N] = 1$ in the asymptotic form of the wave function (17).

F. Dipole-dipole relaxation for fermions

Formula (47) for $1/\tau_k$ is true in general for the relaxation of a particle with spin $\mathbf{S}$ due to a potential of the form (6). We now restrict our derivation to the dipolar interaction where $L = 2$. The solution (22) with the asymptotic behavior (17) does not obey the well-known antisymmetry requirements for a pair of fermions, such as two colliding ^{3}He atoms. One can show the properly antisymmetrized scattering amplitude F_1 has no even partial waves and the amplitude of the odd partial waves is a factor of $\sqrt{2}$ larger than is the case for the potential scattering discussed above. Since the scattering rate is proportional to the square of the scattering amplitude, we should therefore put an additional factor of 2 in the numerator of (47) and exclude even partial waves from the sum. Substituting (10) and the extra factor of 2 into (47), we find

$$\frac{1}{\tau_k} = [N]\frac{24\pi m}{5\hbar^3 k^5}\left(\frac{\mu_I}{I}\right)^4 \times \sum_{l,l'}(2l+1)(2l'+1)C^2(ll'2;00)\left\langle\frac{1}{r^3}\right\rangle^2_{ll'}. \quad (48)$$

The sum extends only over odd values of l and l'.

The thermally averaged spin-relaxation rate is simply

$$\frac{1}{\tau} = \int_0^\infty \frac{P(k)}{\tau_k}dk. \quad (49)$$

The Boltzmann probability distribution of relative momenta is

$$P(k) = \frac{4\pi\hbar^3 k^2}{(2\pi m\kappa T)^{3/2}}\exp\left(\frac{-\hbar^2 k^2}{2m\kappa T}\right), \quad (50)$$

where κ is Boltzmann's constant and T is the absolute temperature.

G. Comparison with previous results

The relaxation rate for ^{3}He (48) is identical to the result of Mullin, Laloë, and Richards [22], although the two derivations are very different. The expression for the relaxation rate derived by Shizgal [19, 20] is identical in form to our result. However, an error appears in the derivation given in Ref. [19] between Eqs. (16) and (24), which leads to the inclusion of an extra factor of $\cos\delta_l \cos\delta_{l'}$ in the matrix element (36). Since the phase shift $\delta_l \to 0$ as $E \to 0$ for $l > 0$ (and for $l = 0$ in the case of ^{3}He), the resulting error will increase with increasing temperature. For ^{3}He, the error in the relaxation rate ranges from -16.4% to -23.8% over the temperature range of 4.2 to 20 K, considered in Refs. [17–20].

III. NUMERICALLY CALCULATED RELAXATION RATES

The evaluation of the relaxation rate $1/\tau$ for ^{3}He involves numerical integration of the Schrödinger equation (29), the relevant matrix elements (36), and the final integral over momentum (49). Three different empirical interatomic potentials $V^{(0)}(r)$ were employed in the calculation of the radial eigenfunctions $g_l(r)$ (see Fig. 1) [21, 32, 33]. Since the relaxation rates calculated with these three interatomic potentials typically differ by only 1–2 %, we performed the numerical calculation of $1/\tau$ to better than 1%.

The $g_l(r)$ are found by numerically integrating the radial Schrödinger equation (29). In practice, the wave function is set to zero well inside the classical turning point, typically at $r_i = 1$ Å. This necessary approximation to the proper initial boundary condition (30) results in a negligible contribution of the undesired solution to (29) in the numerically calculated $g_l(r)$. The Schrödinger equation is integrated outward in r until the interatomic potential is only 0.03% of the kinetic energy of the particle. The numerically calculated wave function is then normalized by matching it and its derivative to that of the free-particle wave function

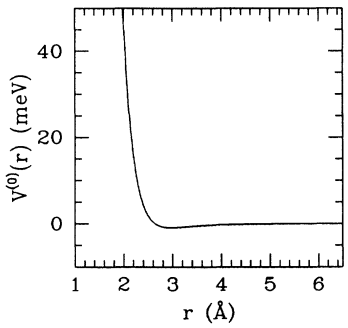

FIG. 1. One of the three different ^{3}He-^{3}He interatomic potentials used in calculating the dipolar relaxation rate. The HFD-B potential of Ref. [21] is shown, but the the mLJ-D potential of Ref. [32] and the ESMSV II potential of Ref. [33] are barely distinguishable from the HFD-B potential on this scale.

$$g_l^{(0)}(r) = kr\left[\cos(\delta_l) j_l(kr) - \sin(\delta_l)\eta_l(kr)\right], \tag{51}$$

where $j_l(x)$ is the spherical Bessel function regular at the origin and $\eta_l(x)$ is the irregular spherical Bessel function. The wave function (51) has the correct behavior for large r (31) and is of course the general solution to the Schrödinger equation (29) for $V^{(0)} = 0$.

The numerical integration was carried out using the Bulirsch–Stoer algorithm as implemented by Press *et al.* [34]. The excellent programs of Ref. [34] are designed to allow good control of any errors which may accumulate in the integration. Reasonable variations in the parameters controlling the integration, the value of r_i, and the conditions for matching $g_l(r)$ to (51) all resulted in changes in $1/\tau_k$ of less than 0.2% over the entire energy range.

With the calculated $g_l(r)$, we numerically integrated the matrix elements $\langle 1/r^3\rangle_{ll'}$ appearing in (48). These matrix elements converged with increasing k or decreasing l to the value

$$\left\langle \frac{1}{r^3} \right\rangle_{ll'} \sim 0.3\frac{k}{r_t^2}, \tag{52}$$

where r_t is the classical turning point for the effective potential of (29). For $l \gg kr_t$, the effective potential of the radial Schrödinger equation (29) is simply the centrifugal barrier potential so that wave function is given by

$$g_l = kr j_l(kr) \tag{53}$$

and need not be calculated numerically. The integration of the matrix elements can then be carried out analytically to find [35]

$$\left\langle \frac{1}{r^3} \right\rangle_{ll} = \frac{k^3}{2l(l+1)} = 0.5\frac{k}{r_t^2}, \tag{54}$$

$$\left\langle \frac{1}{r^3} \right\rangle_{ll+2} = \frac{k^3}{6(l+1)(l+2)}. \tag{55}$$

The differing numerical factors of 0.3 and 0.5 in (52) and (54) are presumably due to the different slopes of the centrifugal barrier and the interatomic potential. The analytical expressions (54) and (55) for the matrix elements for high l allowed us to numerically calculate the sum (48) for $1/\tau_k$ out to arbitrarily large l. (We chose $l = 1001$.)

The relaxation rate (49) was calculated for temperatures from 0.1 to 550 K and is shown in Figs. 2 and 3. As pointed out by Mullin, Laloë, and Richards [22], the minimum at about 1 K occurs because the de Broglie wavelength of the pseudoparticle has become equal to the hard core repulsive potential wall. For temperatures well below 1 K, even the $l = 1$ centrifugal barrier is much larger than the interatomic potential at all r for which the probability amplitude $\psi(\mathbf{r})$ is significant. The relaxation rate then becomes identical to that calculated for $V^{(0)} = 0$. In the Appendix, we show that for $V^{(0)} = 0$ the rate is

$$\frac{1}{\tau} = [N]\frac{32}{\hbar^4}\mu_I^4\sqrt{8\pi m^3\kappa T}\,. \tag{56}$$

In Fig. 3, we see the relaxation rate converge to this value for low temperatures.

IV. EXPERIMENTAL RESULTS

We have made a series of aluminosilicate (Corning No. 1720) glass cells containing 4–12 amagats of ^{3}He gas, 75 Torr of N_2, and a few mg of Rb. (The Rb and N_2 are necessary to polarize the ^{3}He by the method described in Sec. IV B.) In order to observe the bulk dipolar relaxation in ^{3}He, all other relaxation mechanisms must be suppressed. These mechanisms include relaxation due to magnetic field inhomogeneities [36], relaxation on the cell walls due either to the glass surface or to paramagnetic centers on the surface [37–39], and relaxation due to paramagnetic species in the bulk gas. Because relaxation from magnetic field inhomogeneities decreases with increasing pressure, this relaxation was suppressed in our high pressure targets. Although Pyrex glass is depolarizing to ^{3}He, relaxation on aluminosilicate (Corning No. 1720) glass surfaces is very weak and can probably be

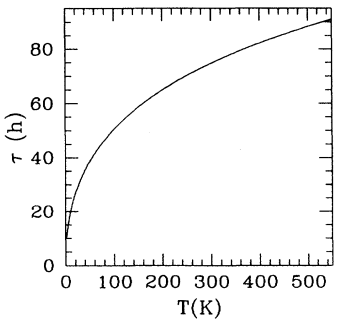

FIG. 2. Temperature dependence of the relaxation time for a 10 amagat polarized ^{3}He sample due to the magnetic-dipole interaction calculated with the HFD-B interatomic potential. The relaxation times calculated using the mLJ-D potential and the ESMSV II potential differ by less than a few percent over the temperature range shown.

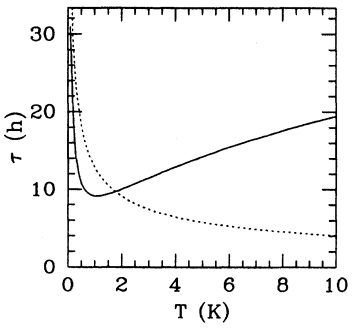

FIG. 3. Low temperature relaxation time for a 10 amagat polarized ^{3}He sample calculated with the HFD-B interatomic potential. The dotted line is the relaxation time (A16) for no interatomic potential. Note that this calculation does not agree with the results of Ref. [18] for the reasons explained in Sec. II G.

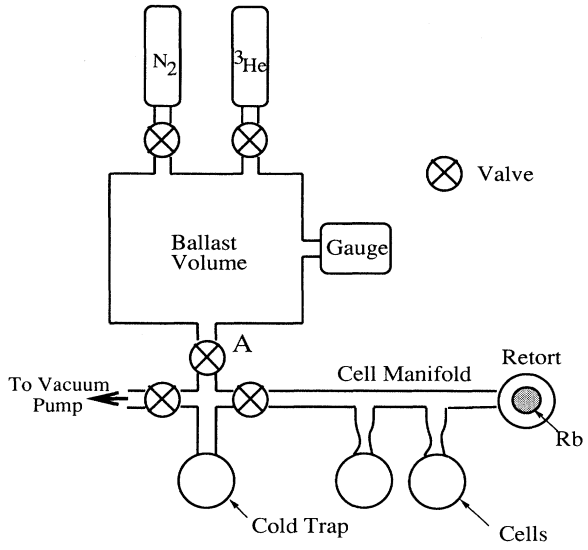

FIG. 4. Schematic of the vacuum system. Below valve *A* the system is all glass. Above and including valve *A*, the system is stainless steel or brass. The pressure gauge is a Baratron model 310CHS-01000, which is accurate to 0.1%.

ascribed to paramagnetic sites on the surface of the glass [39]. Therefore, we were primarily concerned with reducing paramagnetic impurities both on the glass surface and in the filling gases.

A. Cell production

The procedure described here for filling the high pressure cells is an extension of previous methods to produce ^{3}He cells [4, 40, 41]. In this earlier work, the relaxation rates were somewhat unreproducible and were attributed to wall relaxation. On the basis of this work, it appears that if the filling gases are sufficiently clean, and if the interior glass surfaces are hand blown without the aid of forming gases, almost all relaxation is due to the ^{3}He magnetic-dipole interaction. If it is not possible to use freshly reblown glass, a significant reduction in wall relaxation can be achieved by cleaning the glass with HNO_3.

The cells we produced were 1 in. diameter aluminosilicate glass spheres filled with 50 – 100 Torr of 99.9995% pure N_2, 4–12 amagats of ^{3}He [42], and a few milligrams of natural Rb. The vacuum system used to fill the high pressure ^{3}He cells is shown in Fig. 4. The volume of each section in the system was measured to ~1% based on a calibration volume not shown. A glass manifold with two cells was attached to the system and baked out at 450 °C for ~12 h under high vacuum. The cells were then filled with 1–2 Torr of N_2 and an rf discharge was run for about 10 min. The purpose of the discharge was to dislodge any impurities on the walls. We note that there may be evidence that such a discharge actually creates paramagnetic sites on the glass surface [37]. After evacuating the system, natural Rb was distilled from the retort into the cell with a hand torch and N_2 was loaded into the cell manifold.

Perhaps the most important part of the cell making process is the cleaning of the ^{3}He. A small, removable liquid ^{4}He Dewar was constructed which could be clamped around either the trapping region or the cell. The temperature of the Dewar was adjusted by changing the flow of liquid ^{4}He through the Dewar. With the trap region warm, the ballast volume and trap region were filled to about 900 Torr of ^{3}He. Using the liquid ^{4}He Dewar, the trap was cooled to about 5K, pulling a large fraction of the gas into the trap. By cycling the temperature between 5 and 25 K, about 1/4 of the gas was forced into and out of the trap. This created a turbulent flow which both mixed the gas in the ballast and trap regions and decreased the time for a given atom to contact the trap wall. Paramagnetic impurities in the gas were thus frozen out in the trap. After 15–20 cycles, the temperature was raised to ~ 25 K leaving ~ 500 Torr of purified ^{3}He in the ballast volume. The trap was then warmed and evacuated.

In preparation for cell filling, the ^{4}He Dewar was clamped around the cell. The dewar was cooled to ~ 10 K freezing the desired amount of N_2 in the cell. The purified ^{3}He was then let into the manifold. By adjusting the temperature of the Dewar, we regulated the amount of ^{3}He collected in the cell. Since the pressure in the vacuum system was less than 1 atm, the cell could then be *tipped off* from the manifold by heating a constriction in the stem.

The total number of ^{3}He atoms in the cell was taken as the difference between the number of atoms in the system before and after removing the cell, as determined from the ideal gas law. After the cell was filled, its volume was measured to ~1% by determining its buoyancy force in water and applying Archimedes's principle.

B. Experimental ^{3}He relaxation rates

We measured the relaxation rate of ^{3}He gas at room temperature as a function of ^{3}He density. The ^{3}He gas was polarized through spin-exchange collisions with optically pumped Rb vapor [4, 13, 14]. The cells were first heated to ~180 °C to achieve Rb number densities of

$\sim 5 \times 10^{14}$ cm^{-3}. Circularly polarized light from a 4 W Ti:sapphire laser optically pumped the Rb atoms at the D_1 line (795 nm). The N_2 gas was present to avoid radiation trapping which would otherwise limit the Rb polarization. A magnetic field of 10–30 G provided the quantization axis. Over a period of hours, the ^{3}He nuclei became polarized to 10–50% by spin-exchange collisions with the polarized Rb vapor. The cells were then cooled to room temperature, reducing the Rb number density to 10^{10} cm^{-3}. The subsequent decay of the ^{3}He polarization was monitored by measuring the nuclear magnetic resonance adiabatic fast-passage (AFP) signal, which is proportional to the ^{3}He polarization [4]. The relaxation rate Γ for a given cell was determined by fitting the polarization as a function of time to a single decaying exponential.

Over the course of two years, cells were produced from a total of seven manifolds. Shown in Fig. 5 are the relaxation rates as a function of [^{3}He] for cells from six of these manifolds. One of the manifolds is not included since it appears to have been contaminated by impurities. The total relaxation rate Γ is the sum of the bulk dipolar relaxation rate $1/\tau$, indicated by the solid line in Fig. 5, and the relaxation rates due to wall relaxation, paramagnetic impurities, magnetic field inhomogeneities, etc. Therefore it must always be true that $\Gamma > 1/\tau$, which is consistent with the data. The proximity of the data points to the solid line and the fact that all the measured points lie above it indicates that we have consistently produced cells which are completely dominated by dipolar relaxation. In fact, the contribution from other relaxation mechanisms ranges from (18 days)$^{-1}$ to (1 yr)$^{-1}$.

V. CONCLUSION

We have derived the spin-relaxation rate of a polarized nondegenerate Fermi gas due to the magnetic dipole-dipole interaction. A numerical calculation of this relaxation rate for nuclear polarized ^{3}He shows that the relaxation time is about 1 week for a 3 amagat cell. Despite these long relaxation times, we have successfully produced ^{3}He cells whose measured relaxation times are dominated by this fundamental bulk dipolar relaxation.

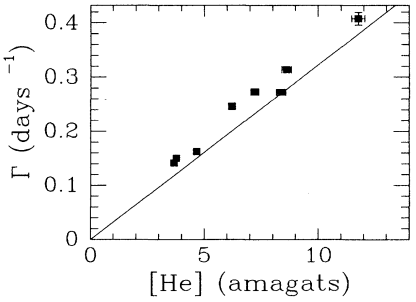

FIG. 5. Experimental relaxation rate as a function of ^{3}He density. No corrections have been applied. The solid line is the numerically calculated dipolar relaxation rate at $T = 23\,^\circ$C. When not shown, the error bars are smaller than the point size.

In a practical sense, our numerical results are important for the production of polarized ^{3}He cells. It is extremely useful to know the ultimate achievable relaxation rate when making and testing polarized ^{3}He cells.

ACKNOWLEDGMENTS

This research was supported by the Air Force Office of Scientific Research Grants Nos. 88–0165 and F49620–92–J–0211.

APPENDIX: RELAXATION RATE OF NONINTERACTING FERMIONS

The previously derived sum (48) for $1/\tau_k$ is of course valid for $V^{(0)} = 0$. With the matrix elements (54) and (55), we could evaluate the sum (48) to find the relaxation rate. However, in this appendix we derive a simpler closed expression.

Consider the limit

$$V^{(0)} = 0, \tag{A1}$$

that is, a gas of spin-1/2 particles with no interaction at all except for the magnetic-dipole–dipole interaction and the requirements of Fermi statistics. We can start with the Born approximation for the scattering amplitude,

$$f(\hat{\mathbf{k}}', \hat{\mathbf{k}}) = \frac{-m}{2\pi\hbar^2} \int e^{-i(\mathbf{k}'-\mathbf{k})\cdot\mathbf{r}'} V^{(1)}(\mathbf{r}') d^3\mathbf{r}'. \tag{A2}$$

To calculate the relaxation of identical, spin-1/2 particles, we need the antisymmetrized scattering amplitude

$$\begin{aligned} F(\hat{\mathbf{k}}', \hat{\mathbf{k}}) &= \frac{1}{\sqrt{2}} \{ f(\hat{\mathbf{k}}', \hat{\mathbf{k}}) - f(-\hat{\mathbf{k}}', \hat{\mathbf{k}}) \} \\ &= \frac{-m}{2\sqrt{2}\pi\hbar^2} \int \left(e^{-i\mathbf{q}\cdot\mathbf{r}} - e^{-i\mathbf{p}\cdot\mathbf{r}} \right) V^{(1)}(\mathbf{r}) d^3\mathbf{r}. \end{aligned} \tag{A3}$$

It is understood here that F refers only to triplet ($S = 1$) scattering. The momentum transfer is $\mathbf{q} = \mathbf{k}' - \mathbf{k}$ and the exchange momentum transfer is $\mathbf{p} = -\mathbf{k}' - \mathbf{k}$. We note that the two types of momentum transfer are orthogonal $\mathbf{q} \cdot \mathbf{p} = 0$.

The irreducible tensor form (10) of the dipole-dipole interaction (3) is not particularly convenient now. Instead we use the equivalent form

$$V^{(1)}(\mathbf{r}) = \left(\frac{\mu_I}{I}\right)^2 (\mathbf{I}_2 \cdot \nabla)(\mathbf{I}_1 \cdot \nabla) \frac{1}{r} = \frac{1}{2} \left(\frac{\mu_I}{I}\right)^2 (\mathbf{S} \cdot \nabla)^2 \frac{1}{r} \tag{A4}$$

since $(\mathbf{I} \cdot \nabla)^2 (1/r) = 0$ for $I = 1/2$. Integrating by parts, we find

$$\begin{aligned} \int e^{-i\mathbf{q}\cdot\mathbf{r}} (\mathbf{S} \cdot \nabla)^2 \frac{1}{r} d^3\mathbf{r} &= -(\mathbf{S} \cdot \mathbf{q})^2 \int \frac{e^{-i\mathbf{q}\cdot\mathbf{r}}}{r} d^3\mathbf{r} \\ &= -4\pi (\mathbf{S} \cdot \hat{\mathbf{q}})^2. \end{aligned} \tag{A5}$$

The antisymmetrized scattering amplitude is therefore

$$F(\hat{\mathbf{k}}',\hat{\mathbf{k}}) = \frac{m}{\sqrt{2}\hbar^2}\left(\frac{\mu_I}{I}\right)^2\{(\mathbf{S}\cdot\hat{\mathbf{q}})^2 - (\mathbf{S}\cdot\hat{\mathbf{p}})^2\}. \quad \text{(A6)}$$

An equivalent expression to (44) for the angle-averaged spin probability current is

$$\dot{Q} = \frac{\hbar k}{4\pi m}\int d^2\hat{\mathbf{k}}\, d^2\hat{\mathbf{k}}'\,\{F|\chi\rangle\langle\chi|F^\dagger - F\,F^\dagger|\chi\rangle\langle\chi|\}\,. \quad \text{(A7)}$$

The rate of change of the spin polarization (15) is therefore

$$\frac{d}{dt}\langle\mathbf{S}\rangle = \frac{km}{8\pi\hbar^3}\left(\frac{\mu_I}{I}\right)^4\int d^2\mathbf{k}\, d^2\mathbf{k}'\langle\chi|\Big\{\left[(\mathbf{S}\cdot\hat{\mathbf{q}})^2 - (\mathbf{S}\cdot\hat{\mathbf{p}})^2\right]\mathbf{S}\left[(\mathbf{S}\cdot\hat{\mathbf{q}})^2 - (\mathbf{S}\cdot\hat{\mathbf{p}})^2\right] - \left[(\mathbf{S}\cdot\hat{\mathbf{q}})^2 - (\mathbf{S}\cdot\hat{\mathbf{p}})^2\right]^2\mathbf{S}\Big\}|\chi\rangle. \quad \text{(A8)}$$

For $S = 1$, $(\mathbf{S}\cdot\hat{\mathbf{q}})^4 = (\mathbf{S}\cdot\hat{\mathbf{q}})^2$. By recoupling the scalar $(\mathbf{S}\cdot\hat{\mathbf{q}})^2$, we find

$$(\mathbf{S}\cdot\hat{\mathbf{q}})^2 = \frac{2}{3} + \sqrt{\frac{8\pi}{15}}\,T_2\cdot Y_2(\hat{\mathbf{q}}). \quad \text{(A9)}$$

Therefore, the squared operator in the second term of the integrand (A8) becomes

$$\begin{aligned}\left[(\mathbf{S}\cdot\hat{\mathbf{q}})^2 - (\mathbf{S}\cdot\hat{\mathbf{p}})^2\right]^2 &= (\mathbf{S}\cdot\hat{\mathbf{q}})^2 - 2(\mathbf{S}\cdot\hat{\mathbf{q}})^2(\mathbf{S}\cdot\hat{\mathbf{p}})^2 + (\mathbf{S}\cdot\hat{\mathbf{p}})^2\\ &= \frac{4}{9} - \frac{16\pi}{75}\Big(T_2\cdot T_2\Big)\Big(Y_2(\hat{\mathbf{q}})\cdot Y_2(\hat{\mathbf{p}})\Big) + \cdots\\ &= \frac{4}{9} - \frac{4}{9}P_2(\hat{\mathbf{q}}\cdot\hat{\mathbf{p}}) + \cdots\\ &= \frac{2}{3} + \cdots, \end{aligned} \quad \text{(A10)}$$

where we have used (43) and the analogous addition formulas for spherical harmonics to obtain the Legendre polynomial P_2 and the other constant coefficients. In the last step, we noted that $\hat{\mathbf{q}}\cdot\hat{\mathbf{p}} = 0$ and therefore $P_2(\hat{\mathbf{q}}\cdot\hat{\mathbf{p}}) = -1/2$. The terms indicated by the dots are either of the form $Y_{2M}(\hat{\mathbf{q}})$ or $\Big[Y_2(\hat{\mathbf{q}})Y_2(\hat{\mathbf{p}})\Big]_{LM}$ with $L > 0$, both of which integrate to zero when (A10) is substituted back into (A8).

We turn now to the first term within the integrand (A8),

$$\begin{aligned}\left[(\mathbf{S}\cdot\hat{\mathbf{q}})^2 - (\mathbf{S}\cdot\hat{\mathbf{p}})^2\right]\,\mathbf{S}\,\left[(\mathbf{S}\cdot\hat{\mathbf{q}})^2 - (\mathbf{S}\cdot\hat{\mathbf{p}})^2\right] &= (\mathbf{S}\cdot\hat{\mathbf{q}})^2\mathbf{S}(\mathbf{S}\cdot\hat{\mathbf{q}})^2 + (\mathbf{S}\cdot\hat{\mathbf{p}})^2\mathbf{S}(\mathbf{S}\cdot\hat{\mathbf{p}})^2\\ &\quad -(\mathbf{S}\cdot\hat{\mathbf{q}})^2\mathbf{S}(\mathbf{S}\cdot\hat{\mathbf{p}})^2 - (\mathbf{S}\cdot\hat{\mathbf{p}})^2\mathbf{S}(\mathbf{S}\cdot\hat{\mathbf{q}})^2. \end{aligned} \quad \text{(A11)}$$

Using (A9) and (45) we find

$$\begin{aligned}(\mathbf{S}\cdot\hat{\mathbf{q}})^2\mathbf{S}(\mathbf{S}\cdot\hat{\mathbf{q}})^2 &= \frac{4}{9}\mathbf{S} + \frac{8\pi}{15}T_2\cdot Y_2(\hat{\mathbf{q}})\mathbf{S}T_2\cdot Y_2(\hat{\mathbf{q}}) + \cdots\\ &= \frac{1}{3}\mathbf{S} + \cdots. \end{aligned} \quad \text{(A12)}$$

There is an analogous expression for (A12) with $\hat{\mathbf{q}} \to \hat{\mathbf{p}}$. We now find the rotationally invariant part of one of the expressions on the right-hand side of (A11)

$$\begin{aligned}(\mathbf{S}\cdot\hat{\mathbf{q}})^2\mathbf{S}(\mathbf{S}\cdot\hat{\mathbf{p}})^2 &= \frac{4}{9}\mathbf{S} + \frac{8\pi}{15}T_2\cdot Y_2(\hat{\mathbf{q}})\mathbf{S}T_2\cdot Y_2(\hat{\mathbf{p}}) + \cdots\\ &= \frac{1}{2}\mathbf{S} + \cdots. \end{aligned} \quad \text{(A13)}$$

Thus, including the results (A10)–(A13) in (A8) and carrying out the integrals over angles, which gives a factor of $(4\pi)^2$, we find

$$\frac{d}{dt}\langle\mathbf{S}\rangle = -\frac{2\pi km}{\hbar^3}\left(\frac{\mu_I}{I}\right)^4\langle\mathbf{S}\rangle. \quad \text{(A14)}$$

This is the relaxation for unit particle number density $[N] = 1$, so the rate for any particle density low enough to ignore Fermi degeneracy is

$$\frac{1}{\tau_k} = [N]\frac{2\pi km}{\hbar^3}\left(\frac{\mu_I}{I}\right)^4. \quad \text{(A15)}$$

The spin relaxation at the temperature T (49) is

$$\frac{1}{\tau} = [N]\frac{32}{\hbar^4}\mu_I^4\sqrt{\pi 8m\kappa T}, \quad \text{(A16)}$$

where we have set $I = 1/2$. This result agrees with the numerical result found by substituting the matrix elements (54) and (55) into the sum (48) and integrating (49).

[1] M. A. Bouchiat, T. R. Carver, and C. M. Varnum, Phys. Rev. Lett. **5**, 373 (1960).
[2] F. D. Colegrove, L. D. Schearer, and G. K. Walters, Phys. Rev. **132**, 2561 (1963).
[3] R. L. Gamblin and T. R. Carver, Phys. Rev. **138**, A946 (1965).
[4] T. E. Chupp, M. E. Wagshul, K. P. Coulter, A. B. McDonald, and W. Happer, Phys. Rev. C **36**, 2244 (1987).

[5] P. L. Anthony *et al.*, Phys. Rev. Lett. **71**, 959 (1993).
[6] K. P. Coulter *et al.*, Nucl. Instrum. Methods Phys. Res. A **288**, 463 (1990); K. P. Coulter, A. B. McDonald, W. Happer, T. E. Chupp, and M. E. Wagshul, *ibid.* **270**, 90 (1988).
[7] G. Greene (private communication).
[8] A. K. Thompson *et al.*, Phys. Rev. Lett. **68**, 2901 (1992); **69**, 391 (1992).
[9] B. Larson *et al.*, Phys. Rev. Lett. **67**, 3356 (1991).
[10] T. E. Chupp and R. J. Hoare, Phys. Rev. Lett. **64**, 2261 (1990).
[11] T. E. Chupp *et al.*, Phys. Rev. Lett. **63**, 1541 (1989).
[12] N. R. Newbury *et al.*, Phys. Rev. Lett. **67**, 3219 (1991); **69**, 391 (1992).
[13] W. Happer, E. Miron, S. Schaefer, D. Schreiber, W. A. van Wijngaarden, and X. Zeng, Phys. Rev. A **29**, 3092 (1984).
[14] X. Zeng, Z. Wu, T. Call, E. Miron, D. Schreiber, and W. Happer, Phys. Rev. A **31**, 260 (1985).
[15] C. l'Huillier and F. Laloë, J. Phys. (Paris) **43**, 197 (1982); **43**, 225 (1982).
[16] C. P. Lusher, M. F. Secca, and M. G. Richards, J. Low Temp. Phys. **72**, 25 (1988).
[17] R. Chapman and M. G. Richards, Phys. Rev. Lett. **33**, 18 (1974).
[18] R. Chapman, Phys. Rev. A **12**, 2333 (1975).
[19] B. Shizgal, J. Chem Phys. **58**, 3424 (1973).
[20] B. Shizgal, Chem. Phys. Lett. **20**, 265 (1973).
[21] R. A. Aziz, F. R. W. McCourt, and C. C. K. Wong, Mol. Phys. **61**, 1487 (1987).
[22] W. J. Mullin, F. Laloë, and M. G. Richards, J. Low Temp. Phys. **80**, 1 (1990).
[23] E. R. Hunt and H. Y. Carr, Phys. Rev. **130**, 2302 (1963).
[24] E. M. Purcell, Phys. Rev. **117**, 828 (1960).
[25] P. A. Franken and H. S. Boyne, Phys. Rev. Lett. **2**, 422 (1959); **3**, 67 (1959).
[26] W. Happer, Rev. Mod. Phys. **44**, 169 (1972).
[27] M. E. Rose, *Elementary Theory of Angular Momentum* (John Wiley, New York, 1957).
[28] A. R. Edmonds, *Angular Momentum in Quantum Mechanics* (Princeton University Press, Princeton, 1957).
[29] D. A. Varshalovich, A. N. Moskalev, and V. K. Khersonskii, *Quantum Theory of Angular Momentum* (World Scientific, Teaneck, NJ, 1988).
[30] I. I. Sobelmann, *Atomic Spectra and Radiative Transitions* (Springer-Verlag, New York, 1979).
[31] Albert Messiah, *Quantum Mechanics* (John Wiley & Sons, New York, 1958), Vol. 1.
[32] H. G. Bennewitz, H. Busse, H. D. Dohmann, D. E. Oates, and W. Schrader, Z. Phys. **253**, 435 (1972).
[33] J. M. Farrar and Y. T. Lee, J. Chem. Phys. **56**, 5801 (1972).
[34] W. H. Press, B. P. Flannery, S. A. Teukolsky, and W. T. Vetterling, *Numerical Recipes* (Cambridge University Press, Cambridge, England, 1990).
[35] I. S. Gradshteyn and I. M. Ryzhik, *Tables of Integrals, Series and Products* (Academic Press, New York, 1980).
[36] G. D. Cates, S. R. Schaefer, and W. Happer, Phys. Rev. A **37**, 2877 (1988); G. D. Cates, D. J. White, Ting-Ray Chien, S. R. Schaefer, and W. Happer, *ibid.* **38**, 5092 (1988).
[37] J. G. Ganiere, Helv. Phys. Acta **46**, 147 (1973).
[38] R. S. Timsit, J. M. Daniels, and A. D. May, Can. J. Phys. **49**, 560 (1971).
[39] W. A. Fitzsimmons, L. L. Tankersley, and G. K. Walters, Phys. Rev., **179** 156 (1969).
[40] K. P. Coulter, Ph.D. thesis, Princeton University, 1989 (unpublished).
[41] B. Larson, O. Häusser, P. P. J. Delheij, D. M. Whittal, and D. Thiessen, Phys. Rev. A **44**, 3108 (1991).
[42] The helium gas was purchased from the Department of Energy and contained 99.8% ^{3}He, 0.2% ^{4}He.